Calculation of temperature effects on the equilibrium crystal shape of Si near (100)

S. Mukherjee and E. Pehlke
Fritz-Haber-Institut der Max-Planck-Gesellschaft, Faradayweg 4-6, D-14195 Berlin (Dahlem), Germany

J. Tersoff
IBM Research Division, Thomas J. Watson Research Center, Yorktown Heights, New York 10598
(Received 26 July 1993; revised manuscript received 18 October 1993)

We present a statistical model of step meandering on small-miscut vicinal Si(100) surfaces, generalized to treat arbitrary azimuth. The model is solved using a transfer-matrix technique and the free energy of the vicinal Si(100) surface is calculated. From the free energy the equilibrium crystal shape is derived at various temperatures. The results are compared with existing experimental data.

I. INTRODUCTION

Step morphology of vicinal Si(100) surfaces containing single-atomic-height (SH) steps has been a subject of intensive recent study.[1–3] This surface exhibits a variety of structures as a function of the miscut angle. Vicinal Si(100) surfaces with a miscut angle smaller than $\sim 1°$ are found to contain only SH steps,[4,5] which alternate between two different kinds, S_A and S_B,[6] depending on whether the dimerization direction in the upper terrace is perpendicular or parallel to the step edge. As the miscut angle further decreases, the terrace widths get larger and the surface can lower its energy by introducing excess steps.[7] This may occur in two different ways, as recent measurements with the low-energy-electron microscope (LEEM) suggest. At very small miscut angles the system decreases the step separation by forming wavy steps.[1] On nominally flat Si(100) surfaces a hill and valley type reconstruction was observed,[2] which we interpret as another mode of introducing steps.[8] The local slope was found to be close to 0.3°.

The occurrence of excess steps on Si(100) with low step density was predicted by Alerhand *et al.*[7] who showed that a sufficiently flat surface could lower its energy by spontaneously forming additional steps to decrease the step separation to a characteristic length l_0. They showed that for straight steps the energy per unit length E_s depends logarithmically on the step separation l,

$$E_s = \lambda_0 - \lambda_\sigma \ln(l/\pi a). \tag{1}$$

Here λ_0 represents the local energy of the step, λ_σ is the strength of the interaction, and a is the lattice constant. At the characteristic step separation l_0, the energy per unit area E_s/l has a minimum, giving

$$l_0 = \pi a \exp(1 + \lambda_0/\lambda_\sigma). \tag{2}$$

It was shown[3] that steps with long-wavelength undulation can also lower the energy by reducing the effective step separation towards the optimum value given by Eq. (2), analogous to the spontaneous step formation proposed by Alerhand *et al.*[7] However, the kinetic barrier for the formation of such structure is expected to be much smaller in the case of the wavy steps, thereby explaining the observation of wavy steps instead of up-down steps (which are energetically preferred) in the experiment.

Another fascinating aspect of the observed surface morphology on Si(100) is a hill and valley structure,[2] which appears when the miscut angle is nominally zero. We believe the hill and valley structure reflects faceting of Si(100). At $T = 0$ one expects a flat Si(100) to facet, with the crystal forming a square pyramid with its apex along (100) and its faces oriented along [011], [01$\bar{1}$], [0$\bar{1}\bar{1}$], and [0$\bar{1}$1] directions.[8] (This assumes that the spontaneous formation of extra up-and-down steps[7] is kinetically forbidden.) At finite temperature the edges between the facets are expected to roughen so that the crystal surface appears to contain conelike hills and holes. Tromp and Reuter[2] have observed precisely such a morphology with LEEM.

Although several calculations of the step structure of SH steps on Si(100) have been reported,[4,5,9] these models are all specialized to [011]-oriented steps, so they cannot be applied to calculate the crystal shape over a range of azimuthal angles, or the related hill-and-valley structures. In this paper we introduce a simple model which can be solved exactly, and with it we calculate the surface free energy of Si(100) at various temperatures as a function of miscut angle θ and azimuth angle ϕ. Our model includes the usual kink and corner energies, and an elastic potential in which the S_A and S_B steps meander. The elastic potential is calculated using continuum elasticity theory with the experimental (anisotropic) elastic constants.[10] The model is solved using a transfer-matrix method, giving the surface free energy.

Inclusion of the azimuth angle allows us to look in detail at the equilibrium crystal shape (ECS), which is obtained from the calculated surface free energy using a Wulff construction. The equilibrium crystal shape is a problem of great interest, yet this is apparently, to our knowledge, the first calculation of ECS for a realistic microscopic model of the surface. Recently the equilibrium shape of small voids in Si has been measured using trans-

mission electron microscopy.[11] This measurement yields a nice picture of the whole ECS of Si, however the detailed structure of the ECS near (100) is difficult to extract. In contrast, the surface structure seen in LEEM, discussed above, may correspond to the ECS near (100), as we assume here.

II. THEORETICAL MODEL AND METHOD OF CALCULATION

A. Model for the step meandering with azimuthal miscut at finite temperature

In this section we outline the model we use to describe the meandering of steps on silicon surfaces oriented arbitrarily, but sufficiently close to (100). The maximum inclination that can be treated by our theory is limited by the appearance of double atomic height steps in the [011] direction. Only single atomic height steps are included in our model, and therefore we consider only small-miscut angles where single atomic height steps dominate.[4]

Previous work dealt with Si surfaces miscut towards [011]. We now generalize to surfaces which are miscut towards an arbitrary direction away from (100). The angle ϕ denotes the azimuthal misorientation, i.e., $\phi = 0°$ corresponds (at zero temperature) to straight S_A and S_B steps running along $[01\bar{1}]$, while $\phi = 45°$ denotes a surface oriented towards [010]. Due to symmetry we can restrict ourselves to $0° \leq \phi \leq 45°$. As in the $\phi = 0°$ case, the direction of dimerization rotates by 90° between adjacent terraces. Therefore, except for the very special situation $\phi = 45°$, there are still two alternating types of steps, in which S_A and S_B segments predominate, respectively. The slope of the surface (i.e., the polar miscut) can be calculated from the periodicity D in the direction normal to the average step edges:

$$\tan\theta = 1/(\sqrt{2}D/a). \tag{3}$$

There are two steps within an interval of length D.

Following the ideas of Alerhand *et al.*[4] and Poon *et al.*,[9] a general two-dimensional model Hamiltonian for M pairs of S_A and S_B steps, each containing N elements of length $2a$ ($2a = 7.6$ Å is the width of one dimer row), is given by

$$\begin{aligned} H = \sum_{j=1}^{M}\sum_{i=1}^{N} & [2\lambda_{\perp}^{A}|h_{i+1}^{A(j)} - h_i^{A(j)}| \\ & + 2\epsilon_c(1 - \delta_{h_{i+1}^{A(j)},h_i^{A(j)}}) + 2\lambda_0^A \\ & + 2\lambda_{\perp}^{B}|h_{i+1}^{B(j)} - h_i^{B(j)}| + 2\epsilon_c(1 - \delta_{h_{i+1}^{B(j)},h_i^{B(j)}}) + 2\lambda_0^B] \\ & + E_{\rm el}(h_1^{A(1)},\ldots,h_N^{A(M)};h_1^{B(1)},\ldots,h_N^{B(M)}). \end{aligned} \tag{4}$$

The position of the ith element in the jth S_A- or S_B-like step is given in units of $2a$ by the integer $h_i^{A(j)}$ or $h_i^{B(j)}$, respectively. The Hamiltonian contains the usual kink energies $\lambda_{\perp}^{A(B)}$ for $S_{A(B)}$ steps, the corner energy ϵ_c, the local step energies $\lambda_0^{A(B)}$, and the elastic relaxation energy $E_{\rm el}$. The local S_A and S_B step energies λ_0^A and λ_0^B have been chosen identical to the kink energies $\lambda_{\perp}^{B}$ and $\lambda_{\perp}^{A}$, for reasons of consistency ($\lambda_0^A = \lambda_{\perp}^{B}$ and $\lambda_0^B = \lambda_{\perp}^{A}$, because locally a kink in an S_A step consists of a portion of an S_B step, and vice versa). Finally, $E_{\rm el}$ denotes the elastic relaxation energy, which is described in more detail in the next subsection.

By enumerating step positions in this way, configurations corresponding to second order ledges (protrusions in a kink, i.e., orthogonal to [011]) have been omitted from the model. However, we know from scanning tunneling microscopy (STM) images that these configurations are in fact extremely rare at $\phi = 0°$. Also for $\phi = 45°$ this approach has been justified *a posteriori* by the observation that most of the kinks in an S_A or S_B step are in fact oriented in the direction of the miscut (see Figs. 1 and 2). Furthermore, we have calculated the difference in free energy between the S_A- and S_B-like step at $\phi = 45°$ (yielding 10^{-3} meV/a^2 at T=600 K), and indeed found it to be negligible compared to typical changes of free energy when the miscut changes. Therefore, at $\phi = 45°$ both S_A and S_B steps are equivalent, as for symmetry reasons they indeed should be. This justifies the validity of our model.

To make the model more tractable, we apply a mean-field-like approximation by taking a certain step and freezing its neighboring step positions, i.e., we calculate the free energy of the whole surface as a sum over free energies of steps which are meandering in a fixed potential. For the results presented below, we have chosen the neighboring steps in such a way that they best approximate straight steps. An example is shown in Fig. 1. At $\phi = 45°$ the step consists of one element of length $2a$ in the [011] direction, one element of the same length in the orthogonal direction, and so on. To check the validity of this ansatz we have calculated the free energy also with other configurations of the neighboring steps, which were much rougher (with kinks of length $4a$ or even longer

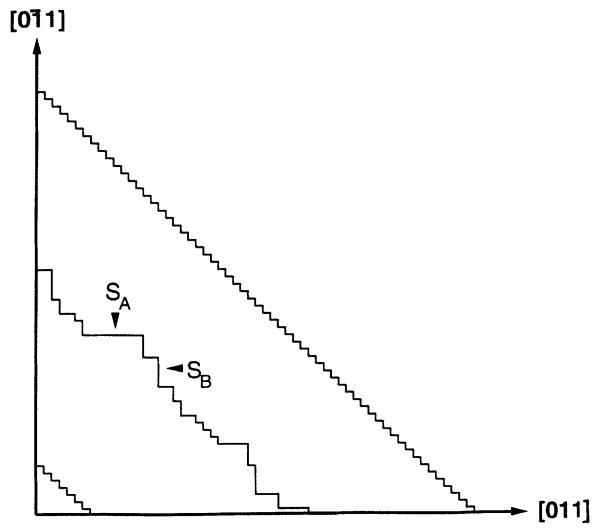

FIG. 1. Schematic drawing of a meandering "S_B-like" step with azimuthal orientation $\phi = 45°$. The neighboring "S_A-like" steps are assumed to be consisting of very fine steps.

kinks). Within reasonable limits for the coarseness of the step, we found no relevant dependency of the result on the form of the neighboring steps.

Using the mean-field-like approach, the Hamiltonian of Eq. (4) can be reduced to two one-dimensional Hamiltonians, one for each type of step,

$$H^A = \sum_{i=1}^{N} [2\lambda_\perp^A |h_{i+1} - h_i| + 2\epsilon_c(1 - \delta_{h_{i+1},h_i}) + 2\lambda_0^A + \epsilon_{\rm el}^A(h_i - h_i^{\rm ref}) + \epsilon_{\rm el}^A(h_{i+1} - h_{i+1}^{\rm ref})], \quad (5)$$

and

$$H^B = \sum_{i=1}^{N} [2\lambda_\perp^B |h_{i+1} - h_i| + 2\epsilon_c(1 - \delta_{h_{i+1},h_i}) + 2\lambda_0^B + \epsilon_{\rm el}^B(h_i - h_i^{\rm ref}) + \epsilon_{\rm el}^B(h_{i+1} - h_{i+1}^{\rm ref})]. \quad (6)$$

In the elastic potential the position of the meandering step is measured with respect to the neighboring step on the left with a reference position $h_i^{\rm ref}$. $\epsilon_{\rm el}$ denotes the elastic relaxation energy per step length a. As in all previous work, the elastic step-step interaction potential derived for straight steps is inserted here (see next subsection).

Note, that by introducing a one-dimensional model we *a priori* exclude the possibility of a *roughening transition*. While such a transition has been proposed for vicinal Si(100) surfaces recently,[12] the experimental results for the deviation-deviation correlation function were not conclusive. We will show below that, up to distances measured in the experiment, the experimental correlation function for S_A steps is in agreement with a correlation function calculated from our one-dimensional model and that they are both consistent with a random-walk picture. Though we cannot answer the question whether there is a roughening transition or not, we can conclude that measurements over longer distances are necessary if one wants to detect a deviation from our simple one-dimensional model. However, what we expect from our model is to give an adequate overall description of the ECS of Si near (100).

B. Elastic relaxation energy

In this section we derive the step-step interaction energy for single-atomic-height steps on Si(100) with an arbitrary azimuthal orientation. The elastic relaxation energy per surface area A can be obtained in a similar way as in the case of straight steps,[7]

$$E_{\rm el}/A = -\tfrac{1}{2} \int_A d^2r\, d^2r' \sum_{i,j=1,2} f_i(\mathbf{r})\, G_{ij}(\mathbf{r} - \mathbf{r}')\, f_j(\mathbf{r}'), \quad (7)$$

where G is the elastic Green's function of the surface and f_i are the two components of the force density parallel to the surface. The force density is obtained from the divergence of the surface stress tensor. To guarantee convergence, the force density (which is given by a sum of δ functions centered at the step edges) is folded with a Lorentzian of width a. This can be imagined as introducing a real-space cutoff close to the step edge within about a lattice constant, where relaxation cannot be described by continuum elasticity theory anyway. Equation (7) can be transformed to reciprocal space, which yields

$$E_{\rm el}/A = -\frac{1}{2} \sum_{\mathbf{q}\neq\mathbf{0}} \sum_{i,j=1,2} f_{\mathbf{q},i}^* \frac{G_{ij}(\phi_q)}{|q|} f_{\mathbf{q},j} \exp(-2a|q|). \quad (8)$$

The sum is over all two-dimensional reciprocal lattice vectors $\mathbf{q}$. $G(\phi_q)$ denotes the angular part of the surface Green function in reciprocal space, and $f_{\mathbf{q}}$ is the Fourier transform of the force density.

We have calculated the surface Green function for Si(100) numerically, taking full account of the anisotropy of the elastic constants. This finally yields

$$E_{\rm el}/A = -\frac{(\sigma_\parallel - \sigma_\perp)^2}{\pi} \{\cos^2\phi\, G_{xx}(\phi) + \sin^2\phi\, G_{yy}(\phi) - \sin\phi\, \cos\phi\, [G_{xy}(\phi) + G_{yx}(\phi)]\} \times \frac{1}{D} \ln\left[\frac{D}{2\pi a} \cos(p\pi/2)\right]. \quad (9)$$

Here p is defined such that $(1+p)D/2$ and $(1-p)D/2$ are widths of the (1×2) and (2×1) terraces, respectively.

To get a deeper understanding of the physical reason behind the ϕ dependence of the elastic relaxation energy, we now calculate this quantity for the special case of an isotropic substrate. In particular, we want to point out that the ϕ dependence does not vanish when the substrate is taken to be isotropic, but that it is in fact due to different modes of relaxation at $\phi = 0°$ and $\phi = 45°$.

For calculating the elastic interaction energy, the atomic roughness of the steps is neglected, and they are described as being straight. In a coordinate system with the x axis oriented perpendicular to the steps the surface stress tensor is given by

$$\sigma = \begin{cases} \sigma_{(1\times2)} & \text{if } 0 \le x < D/2 \\ \sigma_{(2\times1)} & \text{if } D/2 \le x < D \end{cases}, \quad (10)$$

with components

$$\sigma_{(1\times2)} = \begin{pmatrix} \sigma_\parallel \cos^2\phi + \sigma_\perp \sin^2\phi & (\sigma_\perp - \sigma_\parallel)\sin\phi\cos\phi \\ (\sigma_\perp - \sigma_\parallel)\sin\phi\cos\phi & \sigma_\parallel \sin^2\phi + \sigma_\perp \cos^2\phi \end{pmatrix}. \quad (11)$$

A similar expression holds also for $\sigma_{(2\times1)}$, with only the components of the surface stress $\sigma_\parallel$ and $\sigma_\perp$ parallel and perpendicular to the dimer bond being interchanged. For simplicity, steps have been chosen to be equidistant with separation $D/2$. From the divergence of the stress tensor we get the force density

$$\mathbf{f} = (\sigma_\parallel - \sigma_\perp) \begin{pmatrix} \cos(2\phi) \\ \sin(2\phi) \end{pmatrix} [\delta(x) - \delta(x - D/2)]. \quad (12)$$

In reciprocal space for $q \neq 0$ the elastic Green's function of an isotropic substrate is

$$G(q) = \frac{1}{|q|} \begin{pmatrix} \frac{1-\nu}{\mu} & 0 \\ 0 & \frac{1}{\mu} \end{pmatrix}. \quad (13)$$

ν and μ denote Poisson ratio and shear modulus, respectively. (Note that the component of $\mathbf{q}$ parallel to the step edge is zero, so that we are left with an effectively one-dimensional problem.) Carrying out the sum in Eq. (8) we get the result (for $a << D$),

$$E_{\rm el}/A = -\frac{(\sigma_{\parallel}-\sigma_{\perp})^2}{\pi}\frac{1-\nu}{\mu}\left(1+\frac{\nu}{1-\nu}\sin^2(2\phi)\right) \times\frac{1}{D}\ln\frac{D}{2\pi a}. \quad (14)$$

Equation (14) is equivalent to Eq. (9), derived for a special case of equal terrace widths ($p = 0$) and for an isotropic medium. For $\phi = 0°$ the above result further reduces to the expression obtained by Alerhand *et al.*[7] The only difference to their result is the additional factor $[1+\frac{\nu}{1-\nu}\sin^2(2\phi)]$ which leads to a larger energy gain due to relaxation for steps oriented along $\phi = 45°$, compared to those along $\phi = 0°$.

We found the same preference for $\phi = 45°$ also in our complete numerical calculations of $E_{\rm el}$ [Eq. (9)], in which the full anisotropy of the elastic constants is taken into account. However, as demonstrated above, the anisotropy of elastic constants is not a clue to this effect. The ϕ dependence of the elastic relaxation energy can be understood as originating from different step-induced forces at different orientations. At $\phi = 0°$ the forces point in a direction perpendicular to the step edges, resulting in a periodic *compression* and *elongation* in the direction perpendicular to the steps. However, at $\phi = 45°$ the situation is rather different. In this case, the forces are parallel to the average step edges, and the relaxation therefore leads to a *shear* parallel to the steps. The latter relaxation mode results in a more effective stress relaxation at the surface.

C. Free energy and equilibrium crystal shape

The free energy for the one-dimensional Hamiltonian [Eqs. (5) and (6)] describing one step meandering in a given potential can be calculated using standard transfer-matrix techniques. In the following, the indices A and B denoting the type of step are dropped, as the method can be applied in the same way to both steps.

The distance between the meandering step and its neighbor (which is acting as a reference system) is

$$\tilde{h}_i = h_i - h_i^{\rm ref}. \quad (15)$$

This is a rather natural choice of coordinates, because it is the distance $\tilde{h}_i$ which enters into the step interaction potential. According to the construction of the frozen neighboring step there can either be no kink in the reference system at position i (which means $h_{i+1}^{\rm ref} = h_i^{\rm ref}$), or there can be a kink (to the left) of length $2a$ (i.e., $h_{i+1}^{\rm ref} = h_i^{\rm ref} - 1$). Therefore we have to introduce two different transfer matrices. For the first case, $h_{i+1}^{\rm ref} = h_i^{\rm ref}$, we have

$$T_{\tilde{h}_{i+1},\tilde{h}_i} = \exp\{[2\lambda_{\perp}|\tilde{h}_{i+1}-\tilde{h}_i| + 2\epsilon_c(1-\delta_{\tilde{h}_{i+1},\tilde{h}_i}) +2\lambda_0 + \epsilon_{\rm el}(\tilde{h}_{i+1}) + \epsilon_{\rm el}(\tilde{h}_i)]/k_BT\}. \quad (16)$$

In the second case, $h_{i+1}^{\rm ref} = h_i^{\rm ref} - 1$, the shift in the reference system has to be taken into account, by defining another matrix,

$$S_{\tilde{h}_{i+1},\tilde{h}_i} = \exp\{[2\lambda_{\perp}|\tilde{h}_{i+1}-\tilde{h}_i-1| + 2\epsilon_c(1-\delta_{\tilde{h}_{i+1}-1,\tilde{h}_i}) +2\lambda_0 + \epsilon_{\rm el}(\tilde{h}_{i+1}) + \epsilon_{\rm el}(\tilde{h}_i)]/k_BT\}. \quad (17)$$

Here, k_B and T denote the Boltzmann constant and temperature, respectively. The full transfer matrix for the meandering step is a product of such transfer matrices $\mathbf{T}$ and $\mathbf{S}$. We have checked that this product contains the essential properties of a transfer matrix; it can be diagonalized, and the eigenvalue with the largest absolute value is positive and unique. The free energy of a single step is then calculated from the largest eigenvalue $\lambda_{\rm max}$ in the standard way. If the full transfer matrix is formed by m matrices $\mathbf{T}$ and n matrices $\mathbf{S}$, which gives azimuthal miscut angle $\phi = \arctan[n/(n+m)]$, the free energy per projected surface unit cell (with area a^2) is,

$$f(T,\theta,\phi) = -\frac{k_BT}{2(m+n)L}\ln\lambda_{\rm max}. \quad (18)$$

L is the separation of steps in the [011] direction. Finally the total surface energy is calculated from the contributions of both the S_A and the S_B type step.

The ECS of Si(100) for all azimuth angles can be constructed from the free energy per surface unit cell by a Wulff construction.[13] The geometry described by the Wulff construction can be mathematically expressed as[14]

$$r(\hat{\mathbf{h}}) = \min_{\hat{\mathbf{m}}}\left(\frac{\sigma(\hat{\mathbf{m}})}{\hat{\mathbf{m}}\cdot\hat{\mathbf{h}}}\right), \quad (19)$$

where $r(\hat{\mathbf{h}})$ is the distance from the center of the crystal to the surface in the direction $\hat{\mathbf{h}}$. $\sigma(\hat{\mathbf{m}})$ is the free energy per unit area of the surface with orientation $\hat{\mathbf{m}}$. We use spherical coordinates to describe the ECS, in which the previous equation can be expressed as

$$r(\tilde{\theta},\tilde{\phi}) = \min_{\theta,\phi}\left[\frac{\sigma(\theta,\phi)}{\cos\theta\cos\tilde{\theta}[1+\tan\theta\tan\tilde{\theta}\cos(\phi-\tilde{\phi})]}\right]. \quad (20)$$

Here the coordinates θ,ϕ refer to the surface orientation $\hat{\mathbf{m}}$, and $\tilde{\theta},\tilde{\phi}$ to the direction $\hat{\mathbf{h}}$.

III. RESULTS AND DISCUSSION

In this section we present the results obtained from our model for vicinal Si(100) surfaces. For calculating the elastic potential, we have taken the stress anisotropy parameter $\Delta\sigma = 2$ eV/a^2, which is in accordance with results from *ab initio* density-functional theory (DFT) calculations for a (1×2) reconstructed surface.[15,16] The measured[17] value of the surface stress anisotropy, however, is smaller. Very recent DFT results[18,19] suggest this to be due to a stress relaxation in the $c(4\times2)$ or $p(2\times2)$ structure. We will discuss the effect of choosing a smaller stress anisotropy in subsection C below.

The local energies are taken to be λ_0^A =22 meV/a and λ_0^B =66 meV/a. This choice of parameters ensures the minimum in the step energy per unit area of Eq. (1) at $\theta = 0.3°$, which is the local miscut angle of the observed surface morphologies at Si(100).[1,2] Furthermore, these local step energies are in reasonable agreement with the values $\lambda_\perp^B$ =28 meV/a and $\lambda_\perp^A$ =90 meV/a inferred from experiment by Swartzentruber *et al.*[20] The corner energy ϵ_c =40 meV has been directly taken from experiment.[20] The experimental parameters were extracted from STM measurements of the kink length distribution by assuming that the sample is in thermal equilibrium at about 870 K. If the sample actually equilibrates at a lower temperature than was assumed, then the true values of these parameters would be smaller than those inferred.[5]

A. Kink probability

First, we discuss the probability $P(n)$ of having a kink of length n in units of $2a$. $P(n)$ has been measured so far for steps oriented towards [011] ($\phi = 0°$),[5,21] where $P(n)$ is symmetric around $n = 0$. However, the situation is different when the steps have an azimuthal orientation. For steps oriented towards [010] ($\phi = 45°$) $P(n)$ becomes highly asymmetric (Fig. 2). Our transfer-matrix results show that the probability of having kinks in a direction opposite to the miscut direction [011] is almost zero for S_A steps and it is very small for S_B steps.

For the $\phi = 0°$ case, Swartzentruber *et al.*[5] have demonstrated that they can fit their measured data for the kink probability distribution with a simple Boltzmann factor $\exp[-(2\epsilon_c + 2n\lambda_\perp)/k_BT]$. Similarly, we formulate a simple model of freely meandering steps, dropping the elastic interaction terms in the Hamiltonian. In this case the Hamiltonian for a freely meandering step with N positions can be written in terms of kink and corner energies as

$$H_N = \sum_{i=1}^{N} 2\lambda_\perp |n_i| + 2\epsilon_c(1 - \delta_{n_i,0}). \tag{21}$$

The solution of this problem is straightforward even for steps with azimuthal orientation ϕ. We obtain for freely meandering steps the kink probability

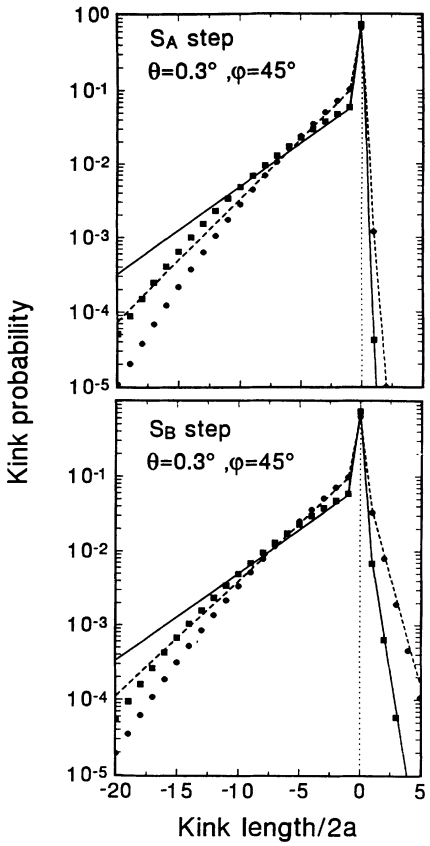

FIG. 2. Kink probability as a function of kink length calculated using the transfer-matrix method for S_A- and S_B-like steps at 400 K (squares) and 600 K (circles). The solid and dashed lines correspond to results obtained using a model of freely meandering steps at the same temperatures. The steps are oriented towards [010] azimuth ($\phi = 45°$) and have a slope 0.3°. The kink length is negative when the kink meanders in the direction of the miscut, and positive when it meanders in the opposite direction.

$$P(n) = \left(1 + \frac{bc\zeta}{1-b\zeta} + \frac{bc}{\zeta - b}\right)^{-1} \cdot \begin{cases} cb^{-n}\zeta^n & \text{if } n < 0 \\ 1 & \text{if } n = 0 \\ cb^n\zeta^n & \text{if } n > 0 \end{cases} . \tag{22}$$

Here, $b = \exp(-2a\lambda_\perp\beta)$, $c = \exp(-2\epsilon_c\beta)$, and $\zeta = \exp(\mu\beta)$, with $\beta = (k_BT)^{-1}$ and μ is the "chemical potential" which fixes the azimuthal orientation ϕ, given by

$$\tan\phi = \left(\frac{1}{(1-b\zeta)^2} - \frac{1}{(\zeta - b)^2}\right) \Big/ \left(\frac{1}{bc\zeta} + \frac{1}{1-b\zeta} + \frac{1}{\zeta(\zeta - b)}\right). \tag{23}$$

The results of $P(n)$ for freely meandering steps (straight lines in Fig. 2) can be compared to the results from the transfer-matrix diagonalization, including elastic interaction between the steps. Similar to Swartzentruber *et al.*,[5] we find very good agreement for kink lengths up to $n \sim 10$, i.e., for all kinks that occur with a relevant probability. At large n, due to step repulsion, the true $P(n)$ gets smaller than the $P(n)$ obtained from the model of freely meandering steps.

Finally, we observe that for $n > 0$ the distribution $P(n)$ depends on both ϵ_c/k_BT and $\lambda_\perp/k_BT$, as the kinks have to be thermally excited. However, for $n < 0$, the exis-

tence of kinks is partially due to azimuthal miscut: they are forced kinks. It is easy to see that if kinks would all be oriented in the direction of the azimuthal miscut, the $\lambda_\perp$ term would lead to only a constant additive term to the energy, and would therefore not influence the statistics of meandering. Accordingly, our $P(n)$ for $n < 0$ becomes almost independent of $\lambda_\perp$. This may allow an experimental determination of ϵ_c independent of $\lambda_\perp$ at $\phi = 45°$.

Note, that due to geometry of the step structure of Si(100) at $\phi = 45°$, both the kink length distribution of the $S_A(S_B)$ step and the kink separation distribution of the $S_B(S_A)$ step are equivalent and as shown in Fig. 2 they can be well described within the independent kink model Eq. (21).

B. Step correlation function and roughening

Recently a STM measurement on the roughening of Si(100) steps has been reported.[12] The authors have measured the deviation-deviation correlation function $G(r) = \langle (h_0 - h_r)^2 \rangle$ for S_A- and S_B-type steps on vicinal Si(100) with miscut angle θ=0.5° towards [011]. The correlation function $G(r)$ for both steps was found to be nearly proportional to r for values up to 20 dimer rows, therefore no indication was found for a roughening transition, which predicts a logarithmic divergence of $G(r)$ above the roughening temperature T_r.[22] This result has been interpreted as essentially a one-dimensional random-walk problem where step interaction is very small. For comparison with experiment, we have calculated $G(r)$ of S_A steps for vicinal Si(100) with $\theta = 0.5°$ and $\phi = 0°$ at 700 K, 800 K, and 900 K (Fig. 3). We find best agreement with the experiment at $T \sim 800$ K. In order to check the influence of parameters we have repeated the calculations for a smaller corner energy $\epsilon_c = 30$ meV,[5] and the experimental stress anisotropy.[17] This choice of parameters yields best agreement of $G(r)$ at a smaller temperature of about 700 K. It was reported recently by Kitamura *et al.*[23] that steps are dynamic even at ~ 600 K; however, Zandvliet *et al.*[12] cooled down their sample rapidly and concluded their freeze-in temperature to be above 600–700 K. A freeze-in temperature down to 700 K is consistent with our calculations.

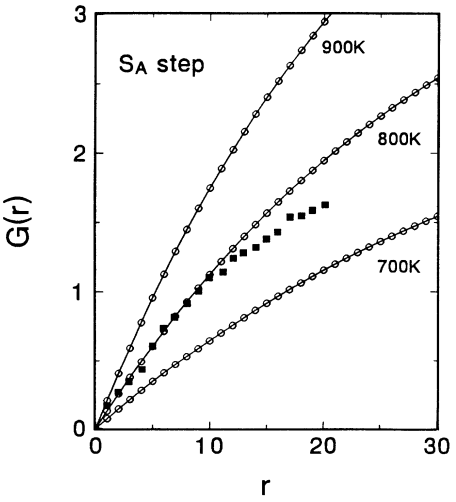

FIG. 3. Deviation-deviation correlation function $G(r)$ of an S_A step edge with $\theta = 0.5°$ and $\phi = 0°$ at different temperatures calculated from transfer-matrix method (open circles). The lines joining the data are for a guide to the eye. Experimental data (filled squares) are taken from Ref. 12. r is in units of $2a$.

Our results indicate a nearly linear behavior of $G(r)$ up to 20 dimer rows. Of course at any temperature our $G(r)$ has to converge for large r, as the steps are confined to the space between their straight left- or right-hand side neighbor. We are aware of the fact that by using a one-dimensional model the steps are not allowed to roughen [i.e., $G(r)$ cannot diverge], however we can conclude that both our and the experimental results can be consistently interpreted as a one-dimensional random walk, in which the step-step interaction is relatively small as compared to the kink formation energies. Measurements over larger step separations r would be necessary to detect a deviation from the simple one-dimensional model, and thereby to decide about the roughening transition on vicinal Si(100) surfaces.

C. Free energy and equilibrium crystal shape (ECS)

We now turn to the free energy and ECS results. In Fig. 4 contour plots of free energy per surface unit cell are shown for temperatures $T = 400$ K, 500 K, and 600 K. At low T the global minimum of the free energy lies along the $\phi = 0°$ axis, while at 500 K another shallow local minimum appears around $\phi = 45°$. Finally, at 600 K and above the situation reverses, when the global minimum shifts towards $\phi \approx 45°$, with only a local minimum remaining at $\phi = 0°$. However, the temperature at which this happens depends on our choice of parameters. In particular, a smaller stress anisotropy would imply a smaller energy preference for $\phi = 45°$, compared to $\phi = 0°$, and hence the shift in the free-energy minimum from $\phi = 0°$ to 45° would occur at a higher temperature.

The contour plots of the free energy support the explanation for the occurrence of wavy steps given previously.[3] The optimum slope (i.e., the optimum polar angle θ) for steps with a given azimuthal orientation is only slightly ϕ dependent. For T=400 K it is $\sim 0.3°$ at $\phi = 0°$ and decreases to $\sim 0.2°$ at $\phi = 45°$. Given a surface with a miscut much smaller than 0.3°, the surface energy [which can be thought of as representing an average of $f(\theta, \phi)$ along the step as long as two-dimensional relaxation is neglected], can be lowered by introducing wavy steps, because locally the slope is increased towards its optimum value. From our free-energy results we can conclude that the local slope should come close to 0.2°–0.3° almost independent of ϕ (insofar as this is not excluded by geometric boundary conditions, such as the average miscut in the [011] direction).

From Fig. 5 we note that at 400 K the ECS appears to be a slightly convex pyramid with faces oriented along

[011] and the directions equivalent by symmetry, i.e., [01$\bar{1}$], [0$\bar{1}\bar{1}$], and [0$\bar{1}$1]. At 500 K new facets near [010], [00$\bar{1}$], [0$\bar{1}$0], and [001] appear, whereas the top of the ECS pyramid remains oriented as in the 400 K case. With our choice of parameters, at 600 K the facets along the diagonal directions dominate, making the top of the ECS pyramid rotate by 45°. The position of the absolute minimum in the free-energy curves remains approximately at a slope angle of 0.3° at all three temperatures (Fig. 4). Therefore, the local slope of the ECS is $\sim$ 0.3° near its top, and the slope increases continuously away from the apex. We show the ECS only up to the point where the slope is 0.6°. At larger angles, double steps begin to play a role,[8] and our model is no longer applicable.

Although Fig. 5 might suggest that the ECS simply consists of a few single facets, this is indeed not the case. The faces of the ECS are in general rounded with respect to both the polar and the azimuthal direction of miscut. We have examined the dependence of the azimuthal orientation ϕ of the faces on the ECS with the direction of

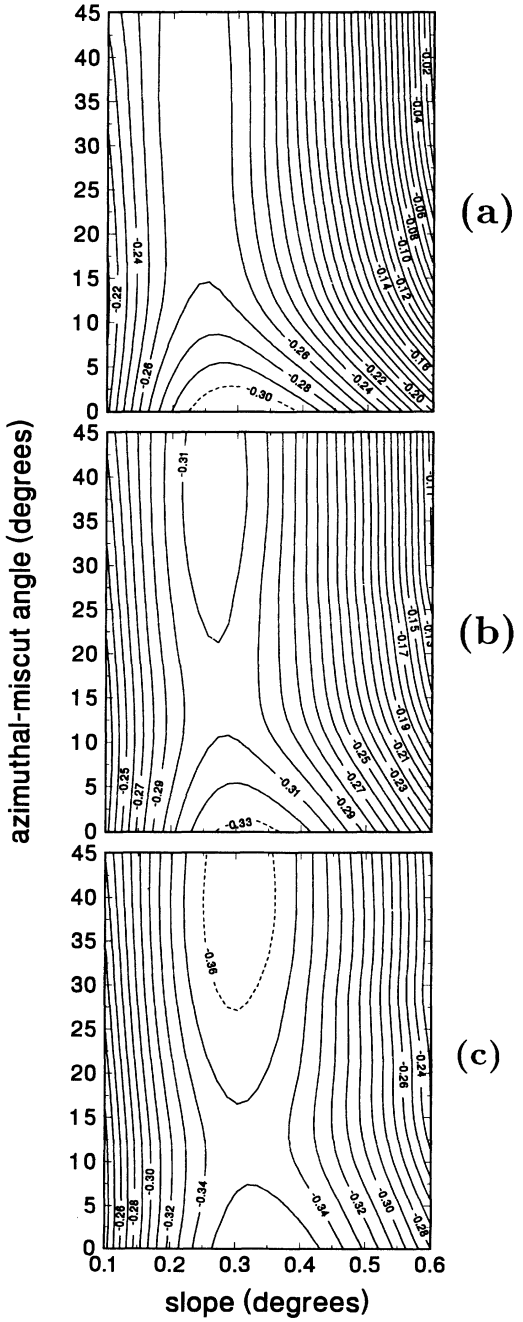

FIG. 4. Free energy per surface unit cell (meV/a^2) of vicinal Si(100) surfaces as a function of slope and azimuthal-miscut angle at (a) 400 K, (b) 500 K, and (c) 600 K. The full elastic potential $\epsilon_{el}(\theta, \phi)$ was used.

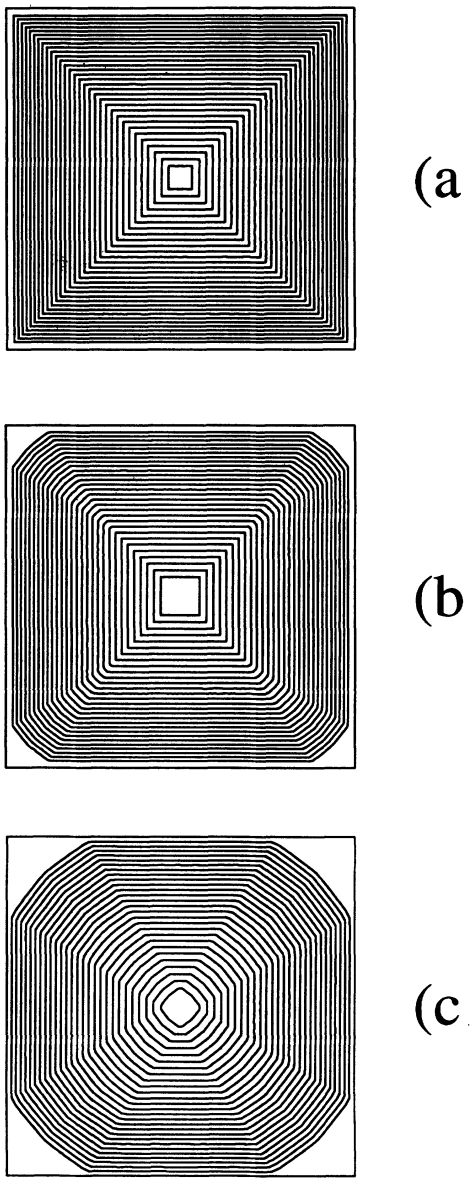

FIG. 5. Equilibrium crystal shape of Si looking down [100], calculated from the free energy data of Fig. 4 using full elastic potential at (a) 400 K, (b) 500 K, and (c) 600 K. Horizontal and vertical directions correspond to [011] and [01$\bar{1}$]. The contours are equidistant in all figures.

view $\tilde{\phi}$ [defined in Eq. (20)], which reveals that the facets are slightly round (i.e., orientation ϕ is varying continuously). In Figs. 5(b) and 5(c) two rounded regions of the ECS with ϕ close to 0° and ϕ large (> 35°) intersect, forming an edge.

The geometry of the ECS is due to the interplay between the ϕ dependence of the geometry factor [denominator of Eq. (20)] and of the free energy. Close to (100), i.e., for small polar angles $\tilde{\theta}$, the geometry factor varies only very slightly, and the orientation of the facets is governed by the global minimum of the free energy. Rounding and facets that correspond to a local but not the global minimum of free energy become visible only for larger $\tilde{\theta}$.

Our ECS results at 600 K are somewhat similar to the rounded shape of the hill-and-valley morphologies observed experimentally on flat Si(100) by Tromp and Reuter.[2] The four edges of the square pyramid are cut by additional facets, making the ECS look round in a global sense. Although the observed morphologies are irregular, their shape is well rounded except at the top or bottom. The shape observed experimentally at the very top (bottom) step of the hill (valley) is essentially due to finite size effects, with the different local energies of S_A and S_B steps leading to an elliptic shape. However, these details have been eliminated from the theory by calculating the thermodynamic limit of infinite system size, and hence the ECS displays the fourfold symmetry of the bulk structure.

Occurrence of new facets along [010], [00$\bar{1}$], [0$\bar{1}$0], and [001] at higher temperatures is essentially due to the azimuth dependence of the elastic interaction potential $\epsilon_{\rm el}(\theta,\phi)$ which has a minimum at $\phi = 45°$. When we drop the azimuth dependence of the elastic potential, using $\epsilon_{\rm el}(\theta,\phi = 0)$ for all ϕ instead, the free energy increases with azimuth rapidly. In Fig. 6, results for the free energy and the corresponding ECS are shown at 900 K for this hypothetical case. We note that even at this high temperature the free energy increases rapidly with azimuthal angle. The ECS appears to be oriented towards [011] azimuth. However, curvature of the facets is visible near the corners. It should be noted that at high temperature the location of the minimum in the free energy moves towards higher polar miscut angle ($\sim 0.5°$), so that the ECS is very flat, consisting of surfaces whose slope changes only slightly. This means that, were it not for the ϕ dependence of the elastic potential, the ECS would be strongly faceted along the [011] azimuth even at quite high temperatures.

As mentioned above, the experimental value of the stress anisotropy is smaller than values from DFT calculations for the Si(100)(1×2) surface. Therefore, we discuss in which way a smaller stress anisotropy would influence the ECS, if the other parameters (local step energies, etc.) are kept constant. For smaller values of stress anisotropy, the optimum polar miscut angle would be much smaller than that which has been observed experimentally.[1] This means that close to (100) the ECS would have a much smaller slope. Moreover, the elastic relaxation energy per step length would get smaller [Eqs. (1) and (2)], while the local step energies

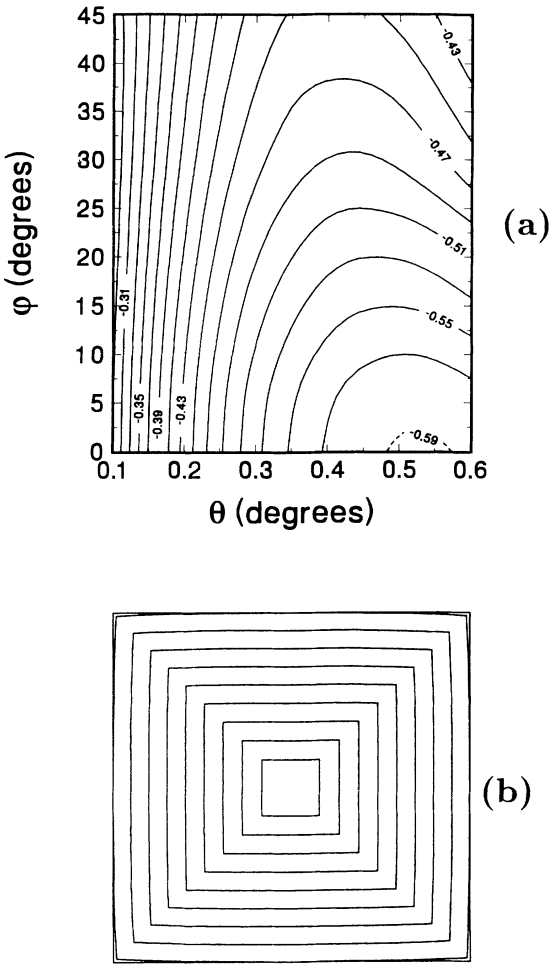

FIG. 6. (a) Free energy per surface unit cell (meV/a^2) of vicinal Si(100) as a function of slope θ and azimuthal-miscut angle ϕ at 900 K. The ϕ-independent elastic potential $\epsilon_{\rm el}(\theta,\phi = 0)$ was used. (b) Equilibrium crystal shape calculated from the free-energy data of (a). The contours are equidistant and the same as in Fig. 5.

stay the same. Therefore, the facets oriented towards $\phi = 45°$ would become less dominant, as they are stabilized by the elastic interaction. Finally, as we start with a small miscut at the top of the ECS, we can proceed to larger directions of view $\tilde{\theta}$ before double height steps appear. In the outer part of the ECS the geometry factor gets more important and leads to a distinct rounding.

IV. SUMMARY

We have presented a one-dimensional model for the meandering of steps on vicinal Si(100) surfaces with arbitrary azimuthal miscut, and derived the ECS from the surface free energy. The azimuth dependence of the elastic step-step interaction potential was found to be crucial for the proper description of the ECS. In fact, whether

facets with orientation $\phi \approx 45°$ appear in the ECS depends on the local step energies (disfavoring $\phi = 45°$ due to the kink energies) counteracting the step interaction potential (which favors $\phi = 45°$ due to the relaxation being more effective for $\phi = 45°$ than at $\phi = 0°$).

ACKNOWLEDGMENTS

We are grateful to R. M. Tromp for providing us his results prior to publication, and would like to thank him and M. Scheffler for stimulating discussions.

[1] R.M. Tromp and M.C. Reuter, Phys. Rev. Lett. **68**, 820 (1992).
[2] R.M. Tromp and M.C. Reuter, Phys. Rev. B **47**, 7598 (1993).
[3] J. Tersoff and E. Pehlke, Phys. Rev. Lett. **68**, 816 (1992).
[4] O.L. Alerhand, A.N. Berker, J.D. Joannopoulos, D. Vanderbilt, R.J. Hamers, and J.E. Demuth, Phys. Rev. Lett. **64**, 2406 (1990).
[5] B. Swartzentruber, N. Kitamura, M.G. Lagally, and M.B. Webb, Phys. Rev. B **47**, 13 432 (1993).
[6] D.J. Chadi, Phys. Rev. Lett. **59**, 1691 (1987).
[7] O.L. Alerhand, D. Vanderbilt, R.D. Meade, and J.D. Joannopoulos, Phys. Rev. Lett. **61**, 1973 (1988).
[8] J. Tersoff and E. Pehlke, Phys. Rev. B **47**, 4072 (1993).
[9] T.W. Poon, S. Yip, P.S. Ho, and F.F. Abraham, Phys. Rev. Lett. **65**, 2161 (1990).
[10] *Semiconductors: Group IV Elements and III-V Compounds*, edited by O. Madelung (Springer-Verlag, Berlin, 1991).
[11] D.J. Eaglesham, A.E. White, L.C. Feldman, N. Moriya, and D.C. Jacobson, Phys. Rev. Lett. **70**, 1643 (1993).
[12] H.J.W. Zandvliet, H. Wormeester, D.J. Wentink, A. van Silfhout, and H.B. Elswijk, Phys. Rev. Lett. **70**, 2122 (1993).
[13] G. Wulff, Z. Kristallogr. Mineral. **34**, 449 (1901).
[14] M. Wortis, in *Chemistry and Physics of Solid Surfaces VII*, edited by R. Vanselow and R. Howe (Springer-Verlag, Berlin, 1988).
[15] M.C. Payne, N. Roberts, R.J. Needs, M. Needels, and J.D. Joannopoulos, Surf. Sci. **211/212**, 1 (1989).
[16] R.D. Meade and D. Vanderbilt, in *Proceedings of the Twentieth International Conference on the Physics of Semiconductors*, edited by E.M. Anastassakis and J.D. Joannopoulos (World Scientific, Singapore, 1990), p. 123.
[17] M.B. Webb, F.K. Men, B.S. Swartzentruber, R. Kariotis, and M.G. Lagally, Surf. Sci. **242**, 23 (1991).
[18] A. Garcia and J.E. Northrup, Phys. Rev. B **48**, 17 350 (1993).
[19] J. Dąbrowski, E. Pehlke, and M. Scheffler, Phys. Rev. B (to be published).
[20] B. Swartzentruber, Y.W. Mo, R. Kariotis, M.G. Lagally, and M.B. Webb, Phys. Rev. Lett. **65**, 1913 (1990).
[21] H.J.W. Zandvliet, H.B. Elswijk, E.J. van Loenen, and D. Dijkkamp, Phys. Rev. B **45**, 5965 (1992).
[22] J. Villain, D.R. Grempel, and J. Lapujoulade, J. Phys. F **15**, 809 (1985).
[23] N. Kitamura, B.S. Swartzentruber, M.G. Lagally, and M.B. Webb, Phys. Rev. B **48**, 5704 (1993).